

Thermodynamics of anion exchange on a chloride-intercalated zinc–aluminum layered double hydroxide: a microcalorimetric study

Yaël Israël^a, Christine Taviot-Guého^b, Jean-Pierre Besse^b, Jean-Pierre Morel^a and Nicole Morel-Desrosiers^{*a}

^a Laboratoire de Thermodynamique des Solutions et des Polymères, UPRESA CNRS 6003, Université Blaise Pascal (Clermont-Ferrand II), 24 avenue des Landais, 63177 Aubière cedex, France. E-mail: nicole.morel@univ-bpclermont.fr

^b Laboratoire des Matériaux Inorganiques, UPRESA CNRS 6002, Université Blaise Pascal (Clermont-Ferrand II), 24 avenue des Landais, 63177 Aubière cedex, France

Received 4th August 1999, Accepted 7th January 2000

Published on the Web 8th February 2000

The thermodynamic properties of anion exchange on a chloride-intercalated zinc–aluminium layered double hydroxide have been studied at 298.15 K. The heats for total exchange of Cl^- for F^- , Br^- , I^- , OH^- , NO_3^- , and SO_4^{2-} have been determined by microcalorimetry and the standard molar enthalpies of these exchange reactions have been estimated. For the processes involving OH^- and NO_3^- , the exchange isotherms have been determined using potentiometry in the former case and capillary ion analysis in the latter. The standard molar Gibbs free energy and entropy changes upon exchange of Cl^- for OH^- and exchange of Cl^- for NO_3^- have been calculated as a function of the fraction of exchanged Cl^- . These exchange processes appear to be entropy-driven, but the selectivity is controlled by the enthalpic contribution.

Introduction

Layered double hydroxides (LDHs), also known as anionic clay materials, display a brucite-type layered structure in which some divalent metallic cations (M^{II}), such as Mg^{2+} , Fe^{2+} , Co^{2+} , Ni^{2+} and Zn^{2+} , are replaced by trivalent metallic cations (M^{III}), such as Al^{3+} , Fe^{3+} and Cr^{3+} , giving rise to positively charged layers balanced by anions (A^{n-}) located in the interlayer space together with water molecules. LDHs are usually formulated as: $[\text{M}^{\text{II}}_{1-x}\text{M}^{\text{III}}_x(\text{OH})_2]^{x+} \cdot [\text{A}^{n-}]_{x/n} \cdot n\text{H}_2\text{O}$ abbreviated hereafter as $[\text{M}^{\text{II}} - \text{M}^{\text{III}} - \text{A}]$. The interlayer anions are easily exchanged (CO_3^{2-} , organo anions, oxo anions ...) and the nature of the layer cations can also be altered (M^{II} : Mg^{2+} , Fe^{2+} , Co^{2+} , Ni^{2+} , Zn^{2+} ...; M^{III} : Al^{3+} , Fe^{3+} , Cr^{3+} ...), offering the possibility of finely modulating the chemical composition of these materials. Presently, there is an intensive search for uses for these materials in heterogeneous catalysis, in separation and membrane technology, filtration, scavenging and controlled release of anions and for electroactive and photoactive materials.^{1–4}

Although the exchange properties of clay minerals have been widely studied,^{3–5} very little is known about the thermodynamic characterization of the exchange process. In fact, most of the thermodynamic studies on clays and soils reported in the literature are restricted to the calculation of equilibrium constants for ion exchange reactions. In any case, most of these studies are concerned with cation exchangers. Very few authors report enthalpies and entropies of ion exchange. In the fifties, Slabaugh,⁶ who treated a sodium bentonite with aliphatic amines, determined the enthalpy for these cation exchanges using microcalorimetry. Almost twenty years later, Vansant and Uytterhoeven⁷ calculated, from their study of the exchange of *n*-alkylammonium ions on sodium montmorillonite at three temperatures, the Gibbs free energy, the enthalpy and the entropy for the exchange reactions. Recently, Doula *et al.*⁸ estimated the Gibbs free energy, the enthalpy and the entropy for potassium–calcium exchange on bentonite samples by measuring the amount of potassium exchanged as a function of temperature, while Reis *et al.*⁹ studied the interactions of monoionic kaolinites with *N,N*-dimethylacetamide and

pyridine using titration calorimetry. Even fewer authors have reported thermodynamic data on LDHs. Among them, Miyata¹⁰ determined the ion-exchange equilibrium constants for hydrotalcite-like compounds of the NO_3^- , Cl^- and SO_4^{2-} forms using ion exchange isotherms and the method described by Gaines and Thomas.¹¹ More recently, using an isothermal microcalorimeter, Dékány *et al.*¹² determined the heats of immersion of surfactant-LDHs in *n*-heptane, benzene, toluene and *n*-propanol.

In this paper we apply titration microcalorimetry to the determination of the enthalpy of anion exchange on a LDH of the $[\text{Zn}-\text{Al}-\text{Cl}]$ type. Exchange data for OH^- , F^- , Br^- , I^- , NO_3^- and SO_4^{2-} are reported. For the processes involving OH^- and NO_3^- the exchange isotherms are also given and the standard molar Gibbs free energy and entropy of anion exchange are calculated.

Experimental

Materials

NaNO_3 , NaI , NaBr , Na_2SO_4 (Merck, *pro analysi*), and NaF (UCB, *pro analysi*) were used without further purification. All the solutions were prepared by weight from either freshly prepared triply-distilled water (for microcalorimetry) or deionized water (for LDH synthesis, potentiometry and capillary ion analysis) which, in both cases, was decarbonated in order to avoid carbonate exchange.

Synthesis of the LDH

A layered double hydroxide of the $[\text{Zn}-\text{Al}-\text{Cl}]$ type with a Zn/Al ratio of 2.09 was prepared using a coprecipitation method similar to that described by Miyata.¹⁰ Deionized and decarbonated water was used along with an inert nitrogen atmosphere. 260 mL of an aqueous solution of the metallic chlorides (0.66 mol dm^{-3} in ZnCl_2 and 0.33 mol dm^{-3} in AlCl_3) was added dropwise to a reactor containing about 200 mL of water, at 25 °C and under magnetic stirring. The pH of the reaction mixture was kept constant at 7.5 ± 0.1 by addition of

2 mol dm⁻³ NaOH. After complete addition of the metallic salts, the reaction mixture was left to age at room temperature for 30 h. Then, the precipitate obtained was washed and centrifuged several times and finally dried at room temperature.

The composition of the precursor was [Zn_{0.677}Al_{0.323}(OH)₂][Cl_{0.297}(CO₃)_{0.013}·0.591H₂O]·0.034CO₂, leading to a molecular weight of 110.5 g mol⁻¹ and a divalent/trivalent metallic ratio of 2.09. The quantity of Cl⁻ was 2.69 × 10⁻³ mol per gram of LDH.

Characterization techniques

The elementary analysis was carried out at the Centre d'Analyses du Centre National de la Recherche Scientifique (CNRS France). Powder X-ray diffraction patterns were recorded using a Siemens D501 X-ray diffractometer with Cu-K α radiation.

Microcalorimetry

The microcalorimetric measurements were performed at 298.15 K using a multichannel microcalorimeter (LKB-Thermometric 2277 Thermal Activity Monitor) equipped with a titration-perfusion vessel. Suurkuusk and Wadsö¹³ have thoroughly described this twin thermopile heat conduction calorimeter and analysed its performance. The stainless steel vessel was charged with 0.83 mL of triply distilled water. A precisely weighed amount, m_{LDH} , of LDH (m_{LDH} varying from 1.5 to 9.5 mg) was added and kept in suspension by stirring. Stepwise titration was carried out by addition of the anionic solution at a molality of either 0.503 mol kg⁻¹ (NaF, NaBr, NaI, NaNO₃, Na₂SO₄) or 0.118 mol kg⁻¹ (NaOH). 15 injections were made for each titration experiment. 14 μ L of the anionic solution was injected in each step using a Lund syringe pump (Thermometric) equipped with a 250 μ L Hamilton syringe fitted with a stainless steel cannula. The power values observed upon titration ranged from 10 to 300 μ W. The thermal response was rather slow: depending on the system studied, 60 to 240 min were required for the signal to return to the baseline after each injection. In order to determine the contributions due to dilution of the anionic solution, each experiment was repeated without LDH and the corresponding heats of dilution were subtracted from the heat effects observed upon titration.

Exchange isotherms

The hydroxide anions were determined by potentiometry using a saturated calomel electrode and a glass electrode calibrated with standard buffers. The exchange reactions were carried out at 298.15 K on suspensions prepared with 8.3 g of water and 30.3, 50.1 or 73.9 mg of LDH. The stepwise titration was performed by addition of 0.07 mL of 0.118 mol kg⁻¹ NaOH solution in each step. For reasons of precision, the amounts of LDH and NaOH used in potentiometry were increased tenfold with respect to those used in microcalorimetry, but the proportion of reagents was unchanged.

The exchange of chloride for nitrate anions was followed by capillary ion analysis (Waters Quanta 4000). Here, the amounts of LDH and NaNO₃ were increased threefold with respect to those used in microcalorimetry. The electrolyte used was a chromate aqueous solution to which was added an osmotic flow modifier (Waters OFM OH⁻) and the pH was adjusted to 8.0 with acetic acid. The sample was introduced by hydrostatic injection and the injection time was fixed to 30 s. A potential of 20 kV, corresponding to an intensity of 18–20 μ A, was applied for 5 min. The detection was realized at 254 nm. Each analysis was repeated 4 or 5 times and the surface of each peak obtained by integration using the Millennium 2010 software (Waters).

Results and discussion

The distance between the successive layers of an LDH is very

Table 1 Basal spacings d_{003} (± 0.05 Å) deduced from the powder X-ray diffraction patterns of the initial LDH in the chloride form ([Zn–Al–Cl]) and of samples collected after titration with different anions

Anion	$d_{003}/\text{\AA}$
Cl ⁻ (initial)	7.75
F ⁻	7.63
Br ⁻	7.79
I ⁻	8.14
OH ⁻	7.26
NO ₃ ⁻	8.66
SO ₄ ²⁻	8.89

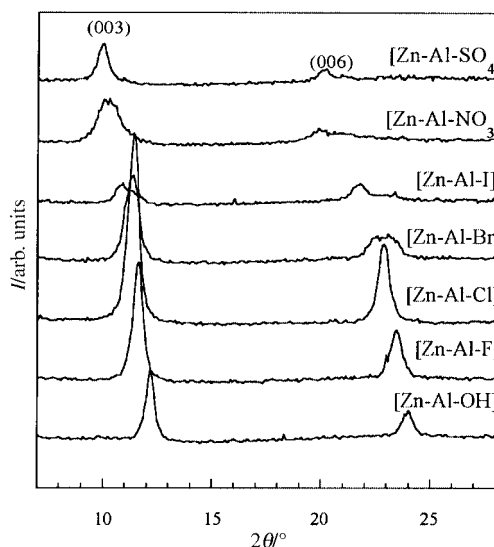
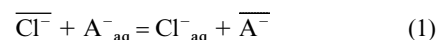


Fig. 1 Powder X-ray diffraction patterns for the LDH in the [Zn–Al–Cl] initial form and in the [Zn–Al–A] forms after titration with different A⁻ anions: F⁻, Br⁻, I⁻, OH⁻, NO₃⁻ and SO₄²⁻.

sensitive to the shape and charge density of the intercalated anion. Powder X-ray diffraction patterns of samples collected after microcalorimetric titration are shown in Fig. 1. From the basal spacings reported in Table 1, which correspond to those observed in the literature,¹⁴ it can be inferred that upon titration the interlayer chloride anions are completely exchanged for the solution anions (A⁻). Additionally, the interlayer distances show no evidence that carbonate exchange has occurred.

The process studied here can thus be described as



where $\overline{\text{Cl}^-}$ and $\overline{\text{A}^-}$ refer to the anions in the LDH solid phase and Cl^-_{aq} and A^-_{aq} refer to the anions in the aqueous solution. This process is characterized by a thermodynamic equilibrium constant, defined as

$$K = \frac{a_{\text{Cl}^-} \overline{a_{\text{A}^-}}}{a_{\text{A}^-} \overline{a_{\text{Cl}^-}}} = \frac{[\text{Cl}^-] \gamma_{\text{Cl}^-} \bar{x}_{\text{A}^-} \bar{f}_{\text{A}^-}}{[\text{A}^-] \gamma_{\text{A}^-} \bar{x}_{\text{Cl}^-} \bar{f}_{\text{Cl}^-}} \quad (2)$$

where a is the activity of the ion in the aqueous solution, \bar{a} is the activity of the ion in the LDH, the term in brackets is the concentration of the ion in solution (expressed in molarity), γ is the activity coefficient of the ion in solution, with the standard state corresponding to the infinitely dilute solution, \bar{x} is the molar fraction of the ion in the LDH and \bar{f} is the activity coefficient of the ion in the LDH with the standard state corresponding to a solid phase containing only one kind of anion in the interlayer domain. For a monovalent–monovalent exchange in a dilute solution of strong electrolytes, the ratio $\gamma_{\text{Cl}^-}/\gamma_{\text{A}^-}$ is close to unity. The process is also characterized by $\Delta_r H^\circ$, the standard molar enthalpy of ion exchange, which corresponds to the total molar heat of exchange.

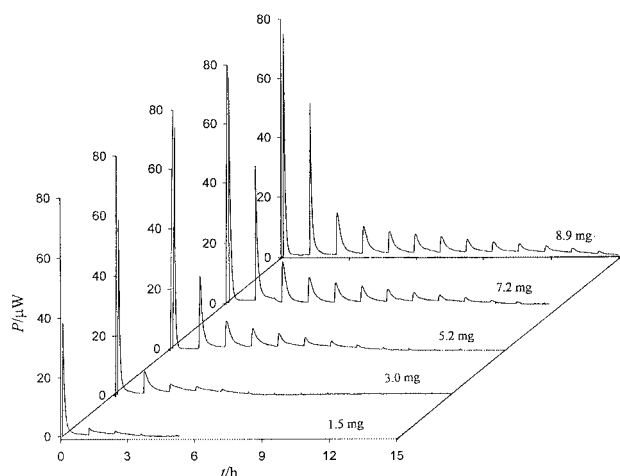


Fig. 2 Calorimetric records (power versus time) for the stepwise addition of aqueous NaOH solution ($0.118 \text{ mol kg}^{-1}$) to different amounts of LDH suspended in water.

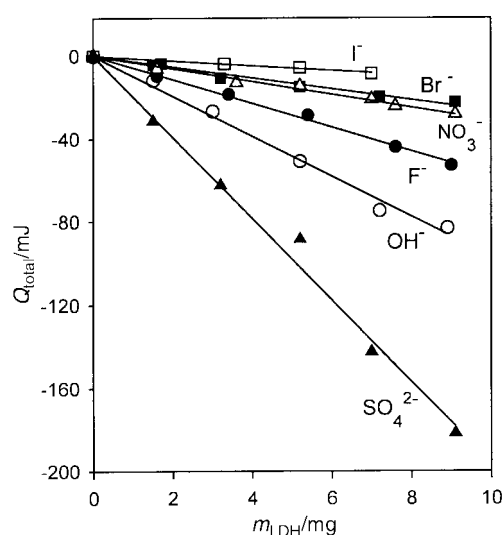


Fig. 3 Variation of the heat value for total exchange with the amount of LDH when chloride is exchanged for fluoride (●), bromide (■), iodide (□), hydroxide (○), nitrate (△) or sulfate (▲).

Fig. 2 shows, as an example, the results of the titration experiments involving stepwise addition of NaOH solution to different amounts of LDH suspended in water. The titration curve becomes flatter as the amount of LDH decreases. For a given amount of LDH, the gradual decrease of the area under the power–time curve corresponds to the progressive exchange of the chloride anions from the LDH for the hydroxide anions of the solution. After a while, no further thermal effect is observed, due to the fact that the anionic exchange is complete, as evidenced by the powder X-ray diffraction patterns of the samples collected after titration. The thermograms show that the process is slow. The heat effects solely due to the exchange process are obtained by correcting the data for the dilution of the anionic solution using the titration experiments carried out without LDH.

The heat value for total exchange, Q_{total} , is obtained by summing-up the corrected heat quantities for the different titration steps. The dependence of Q_{total} on the amount of LDH present when chloride is exchanged for fluoride, bromide, iodide, hydroxide, nitrate or sulfate is shown in Fig. 3. Linear dependence is observed in each case. This confirms that the thermal effect is proportional to the amount of LDH and that the exchange is total in each case. The slope corresponds to the heat effect per mg of LDH. Since each gram of the studied LDH contains 2.69 mmol of chloride anions, the standard

Table 2 Calorimetric study of the Cl^- – A^- exchange on a LDH of the [Zn–Al–Cl] type at 298.15 K: heat value for the total exchange, Q_{total} (mJ mg^{-1}), and standard molar enthalpy change for the exchange reaction, $\Delta_r H^\circ$ (kJ mol^{-1})

A^-	Q_{total}	$\Delta_r H^\circ$
F^-	-5.7 ± 0.2	-2.1 ± 0.1
Br^-	-2.7 ± 0.1	-0.99 ± 0.04
I^-	-1.2 ± 0.1	-0.44 ± 0.02
OH^-	-9.7 ± 0.3	-3.6 ± 0.1
NO_3^-	-3.5 ± 0.2	-1.3 ± 0.1
SO_4^{2-}	-19.7 ± 0.5	-7.3 ± 0.2

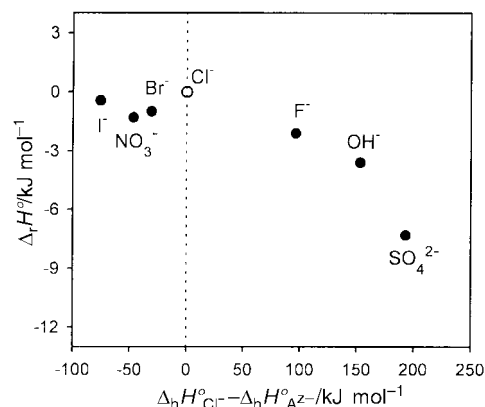


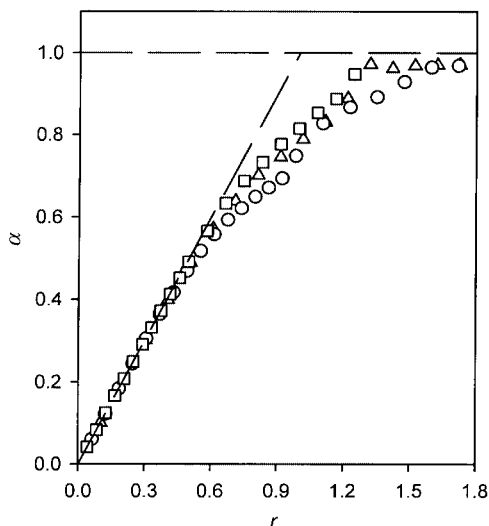
Fig. 4 Variation of the standard molar enthalpy of Cl^- – A^- exchange with the standard molar enthalpy of hydration of Cl^- minus that of A^- .¹⁵

molar enthalpy change, $\Delta_r H^\circ$, for the exchange reaction can be estimated. The values are reported with estimated standard errors in Table 2. The $\Delta_r H^\circ$ values for the anion exchanges studied here, which are rather small and all negative, follow the sequence $\text{SO}_4^{2-} < \text{OH}^- < \text{F}^- < \text{NO}_3^- < \text{Br}^- < \text{I}^-$, similar to that given by Miyata¹⁰ for the ion exchange equilibrium constants for LDHs of the [Mg–Al–A] type, that is $\text{SO}_4^{2-} \approx \text{OH}^- > \text{F}^- > \text{Cl}^- > \text{Br}^- > \text{NO}_3^- > \text{I}^-$.

One would expect the modification of the hydration of the anions to play a role in the exchange process. Thus, we have plotted the $\Delta_r H^\circ$ values obtained for the exchange of Cl^- for A^- against the standard molar enthalpy of hydration of Cl^- minus that of A^- (Fig. 4). This choice is based on the fact that A^- is, to some extent, dehydrated upon intercalation whereas Cl^- is hydrated upon its release from the LDH. There is, however, no way to take into account the extent of hydration or dehydration of each anion. No clear correlation is observed but two families can be identified: the strongly hydrated anions (F^- , OH^- , SO_4^{2-}), which are located to the right of Cl^- in Fig. 4, display the most negative enthalpies of anion exchange whereas the anions located on the other side (Br^- , I^- and NO_3^-), which are slightly less hydrated than Cl^- , yield slightly negative enthalpies of anion exchange. Obviously, the term $(\Delta_h H^\circ_{\text{Cl}^-} - \Delta_h H^\circ_{\text{A}^-})$, which happens to be positive for F^- , OH^- and SO_4^{2-} , cannot contribute significantly to the $\Delta_r H^\circ$ values obtained for these ions. This is in agreement with the fact that the anion remains strongly hydrated upon intercalation. In fact, it is well-known that a significant amount of water is present in the inter-layer domain, as evidenced by X-ray diffraction data,¹ quasi-elastic neutron scattering measurements,¹⁶ and computational simulations.¹⁷ Some authors even consider that the interlayer domain presents a quasi-liquid state.^{18,19} On the other hand, one can imagine that small ions such as F^- and OH^- , or divalent ions such as SO_4^{2-} , interact more strongly than the other anions with the positive sites of the LDH layers. It must be noted, however, that this cannot explain what is observed here since the enthalpies of ion-pairing are generally positive. Thus, it

Table 3 Standard molar thermodynamic quantities (kJ mol⁻¹) characterizing the anion exchange on a LDH of the [Zn–Al–Cl] type at 298.15 K

Anion exchange	log <i>K</i>	Δ _r <i>G</i> [°]	Δ _r <i>H</i> [°]	<i>T</i> Δ _r <i>S</i> [°]
Cl ⁻ → OH ⁻	1.8 ± 0.3	-10 ± 2	-3.6 ± 0.1	6 ± 2
Cl ⁻ → NO ₃ ⁻	-0.63 ± 0.07	3.6 ± 0.4	-1.3 ± 0.1	-4.9 ± 0.5

**Fig. 5** Cl⁻–OH⁻ exchange isotherms: variation of *a*, the fraction of exchanged Cl⁻, with *r*, the ratio of the total number of moles of OH⁻ over the total number of moles of Cl⁻ present in the two phases at equilibrium, for various amounts of LDH [(Δ) 30.3; (○) 50.1 and (□) 73.9 mg].

appears that the sign of the enthalpies of ion exchange is not simple to explain.

The exchange isotherms have been determined for two of the studied anions located to both sides of Cl⁻ in Fig. 4, that is OH⁻ and NO₃⁻. As an example, the results for the Cl⁻–OH⁻ exchange are shown in Fig. 5 where *a*, the fraction of exchanged Cl⁻, that is, *x*_A⁻, is plotted *versus* the ratio of the total number of moles of OH⁻ over the total number of moles of Cl⁻ present in the two phases at equilibrium. The apparent partition constant *K'*, which is given by

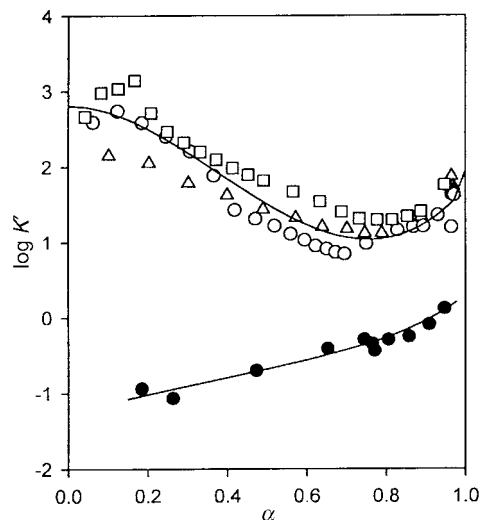
$$K' = \frac{[\text{Cl}^-]_{\text{A}^-} x_{\text{A}^-}}{[\text{A}^-] x_{\text{Cl}^-}} \quad (3)$$

can thus be estimated as a function of *a*: the results obtained for the two processes studied here are shown in Fig. 6. The thermodynamic equilibrium constant may be calculated, following the method of Gaines and Thomas,¹¹ by averaging the apparent partition constant over the entire range of composition of the exchanger

$$\log K = \int_0^1 \log K' da \quad (4)$$

This method, fully described by Gaines and Thomas,¹¹ has been widely used for the thermodynamic study of exchange in clays and soils.^{5,7,10,20} The log *K* values thus deduced are given in Table 3, along with the corresponding standard molar Gibbs energies. Combining these with the Δ_r*H*[°] values of Table 2 yields the standard molar entropies of anion exchange.

In both cases, the exchange process is controlled by the entropic term, which happens to be favourable for the Cl⁻–OH⁻ exchange, but unfavourable for the Cl⁻–NO₃⁻ exchange. The negative entropy observed for the Cl⁻–NO₃⁻ exchange is possibly due to the fact that the nitrate anion, which is forced to adopt an arrangement which favours the closest possible packing, loses most of its degrees of freedom upon intercalation:

**Fig. 6** Variation of *K'*, the apparent partition constant, with *a*, the fraction of exchanged Cl⁻, for the two processes studied here: Cl⁻–OH⁻ exchange on 30.3 (Δ), 50.1 (○) and 73.9 mg (□) of LDH; Cl⁻–NO₃⁻ exchange on 15.6 mg of LDH (●).

computational simulation of a layered double hydroxide of the type [Mg–Al–NO₃] has indeed shown that the nitrate anions must tilt away from coplanarity with the metal hydroxyl sheets in order to minimize important steric repulsions, the layers then being pushed apart.¹⁷ Of course, while the nitrate anions lose degrees of freedom upon intercalation, the expelled chloride anions gain mobility in the solvent. However, the fact that the entropy of exchange is negative seems to indicate that the former effect prevails over the latter. By contrast, the positive entropy for the Cl⁻–OH⁻ exchange is probably due to the similarity of the hydroxyl anions to the intercalated water molecules (diameter, hydrogen bonding). This similarity has been used^{1,10,21} to explain the fact that the LDH in the hydroxyl form shows the best close-packed arrangement, as evidenced by the basal spacings given in Table 1. Because of this, the hydrated hydroxyl ion that goes from the bulk solvent into the interlayer domain of the LDH does not have to lose as many degrees of freedom as NO₃⁻. The positive entropy of exchange seems to indicate that the entropy gained by the expelled Cl⁻ exceeds that lost by the intercalated OH⁻.

On the other hand, the anionic selectivity of a LDH seems to be governed by the enthalpic term, as was shown above by comparison of the sequences respectively followed by our Δ_r*H*[°] values and by the *K* values reported by Miyata.¹⁰ Similar behaviour was observed with bentonite and montmorillonite, for which it was shown^{6,7} that the cation exchange properties are controlled by entropic effects.

In Fig. 7, we have plotted the cumulative heat value at each calorimetric titration step *versus* the corresponding number of moles of exchanged chloride deduced from the Cl⁻–OH⁻ exchange isotherms (for three experiments involving different amounts of LDH) and from the Cl⁻–NO₃⁻ exchange isotherm. Whatever the amount of LDH, *Q* decreases smoothly as the chloride anion is exchanged. Because the heat increments for the last points of each curve are very small, a *pseudo-plateau* is reached before all the interlayer Cl⁻ has been replaced.

We have determined the values of the derivative, d*Q*/d*n*_{Cl-aq}, which in fact corresponds to the molar enthalpy of reaction Δ_r*H*, using the different curves in Fig. 7. These values have been

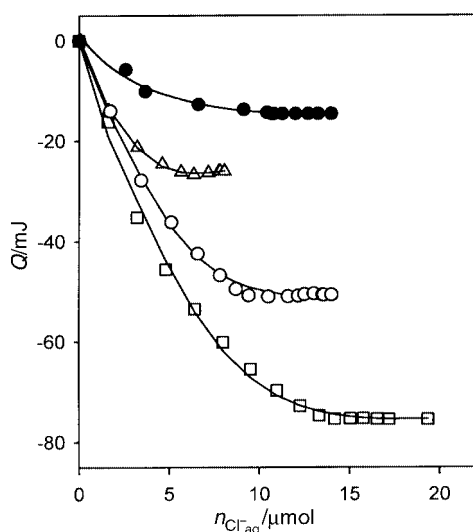


Fig. 7 Variation of the cumulative heat value at each calorimetric titration step with the corresponding number of moles of exchanged chloride deduced from the $\text{Cl}^{-}\text{--OH}^{-}$ exchange isotherms, for three experiments involving different amounts of LDH [(Δ) 3.0; (\circ) 5.2 and (\square) 7.3 mg], and from the $\text{Cl}^{-}\text{--NO}_3^{-}$ exchange isotherm [(\bullet) 5.2 mg of LDH].

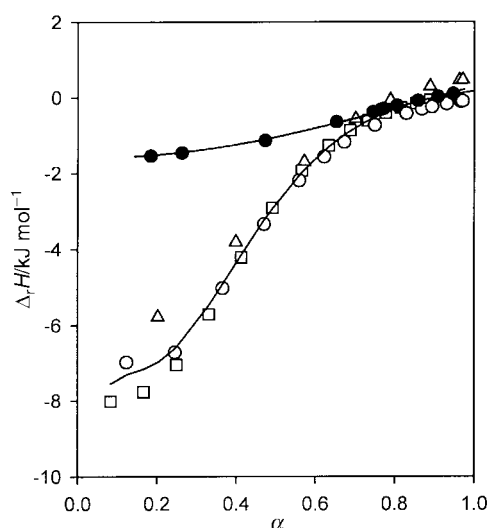


Fig. 8 Variation of the derivative, $dQ/dn_{\text{Cl}^{-}_{\text{aq}}}$, i.e. the molar enthalpy of reaction $\Delta_r H$, with α , the fraction of exchanged Cl^{-} , for the two processes studied here: $\text{Cl}^{-}\text{--OH}^{-}$ exchange on 3.0 (Δ), 5.2 (\circ) and 7.3 mg (\square) of LDH; $\text{Cl}^{-}\text{--NO}_3^{-}$ exchange on 5.2 mg of LDH (\bullet).

plotted as a function of α in Fig. 8. For the $\text{Cl}^{-}\text{--OH}^{-}$ exchange, a unique curve is obtained that shows the variation of $\Delta_r H$ with the fraction of exchanged Cl^{-} . The $\Delta_r H$ values calculated for the $\text{Cl}^{-}\text{--NO}_3^{-}$ exchange are much smaller than those obtained for the $\text{Cl}^{-}\text{--OH}^{-}$ exchange, but the shape of the curve is similar. The fact that $\Delta_r H$ tends towards zero as the fraction of exchanged Cl^{-} approaches unity is due to the existence of the *pseudo-plateau*, as explained above, and cannot be considered a real limit. The S-shape variation can be attributed to the structural change of the exchanger whose interlayer domain goes progressively from a chloride to a hydroxide or nitrate form. When more than 70% of the chloride anion has been exchanged, very weak values of $\Delta_r H$ are observed: it looks as if each additional OH^{-} or NO_3^{-} can then penetrate into the exchanger with almost no energy expenditure because the LDH is already in the hydroxyl or nitrate form.

The corresponding $T\Delta_r S$ values have also been calculated by combining the $\Delta_r G$ values deduced from Fig. 6 and the $\Delta_r H$ values of Fig. 8; they have been plotted as a function of α in Fig. 9. The $T\Delta_r S$ values for the $\text{Cl}^{-}\text{--OH}^{-}$ exchange, which are positive over the whole range of α , show a minimum when

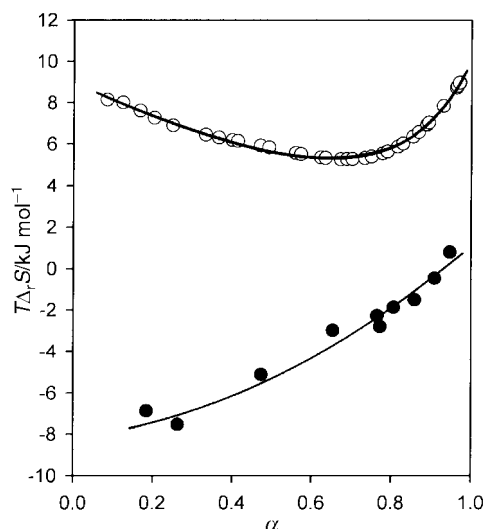


Fig. 9 Variation of $T\Delta_r S$ with α , the fraction of exchanged Cl^{-} , for the two processes studied here: $\text{Cl}^{-}\text{--OH}^{-}$ exchange (\circ); $\text{Cl}^{-}\text{--NO}_3^{-}$ exchange (\bullet).

about 70% of the chloride anion has been exchanged. The entropic contribution appears to become slightly less favourable as the LDH interlayer content goes from 100% Cl^{-} to a mixture of 30% Cl^{-} and 70% OH^{-} . Beyond that, the entropic contribution becomes more and more favourable. Fig. 8 and 9 show that it is at the beginning of the $\text{Cl}^{-}\text{--OH}^{-}$ exchange that the enthalpic and entropic contributions are the most favourable. As the exchange proceeds, these two contributions become less favourable. Above 70% exchange, the process appears to be solely entropic. On the contrary, $T\Delta_r S$ for the $\text{Cl}^{-}\text{--NO}_3^{-}$ exchange is negative and tends progressively towards zero or a slightly positive value as the extent of exchange increases. At the beginning of the $\text{Cl}^{-}\text{--NO}_3^{-}$ exchange, the enthalpic contribution is the most favourable, whereas the entropic contribution is the most unfavourable. As the exchange proceeds, the two contributions tend to zero. As a result, the exchange of Cl^{-} for NO_3^{-} is, on the whole, unfavourable (Table 3). The thermodynamic behaviours observed here for the $\text{Cl}^{-}\text{--OH}^{-}$ and $\text{Cl}^{-}\text{--NO}_3^{-}$ exchanges are fully consistent with the fact that NO_3^{-} loses most of its degrees of freedom upon intercalation, whereas OH^{-} , because of its similarity to the intercalated water molecules, forms the best close-packed arrangement, as evidenced by the structural data^{1,3,10,16,21} and computational simulations.¹⁷

References

- 1 A. de Roy, C. Forano, K. El Malki and J. P. Besse, in *Synthesis of Microporous Materials*, ed. M. L. Ocelli and H. E. Robson, Van Nostrand-Reinhold, New York, 1992, vol. 2, pp. 108–169 and references therein.
- 2 F. Cavani, F. Trifiro and A. Vaccari, *Catal. Today*, 1991, **11**, 173.
- 3 F. Trifiro and A. Vaccari, in *Comprehensive Supramolecular Chemistry*, ed. J. L. Atwood, J. E. D. Davies, D. D. Mac Nicol, F. Vögtle, J. M. Lehn, G. Alberti and T. Bein, Pergamon, Oxford, 1996, pp. 251–291.
- 4 V. Rives and M. A. Ulibarri, *Coord. Chem. Rev.*, 1999, **181**, 61.
- 5 A. Clearfield, *Chem. Rev.*, 1988, **88**, 125.
- 6 W. H. Slabaugh, *J. Phys. Chem.*, 1954, **58**, 162.
- 7 E. F. Vansant and J. B. Uytterhoeven, *Clays Clay Miner.*, 1972, **20**, 47.
- 8 M. Doula, A. Ioannou and A. Dimirkou, *Commun. Soil Sci. Plant Anal.*, 1995, **26**, 1535.
- 9 A. S. Reis, J. de Alencar Simoni and A. P. Chagas, *J. Colloid Interface Sci.*, 1996, **177**, 1.
- 10 S. Miyata, *Clays Clay Miner.*, 1983, **31**, 305.
- 11 G. L. Gaines and H. C. Thomas, *J. Chem. Phys.*, 1953, **21**, 714.
- 12 I. Dékány, F. Berger, K. Imrik and G. Lagaly, *Colloid Polym. Sci.*, 1997, **275**, 681.
- 13 J. Suurkuusk and I. Wadsö, *Chem. Scr.*, 1982, **20**, 155.

- 14 A. de Roy, J. P. Besse and P. Bondot, *Mater. Res. Bull.*, 1985, **20**, 1091.
15 Y. Marcus, *Ion Solvation*, Wiley, Chichester, 1985.
16 W. W. Kagunya, *J. Phys. Chem.*, 1996, **100**, 327.
17 A. M. Aicken, I. S. Bell, P. V. Coveney and W. Jones, *Adv. Mater.*, 1997, **9**, 496.
18 M. Lal and A. T. Howe, *J. Chem. Soc., Chem. Commun.*, 1980, 737.
19 R. Allmann, *Acta Crystallogr., Sect. B*, 1968, **24**, 972.
20 R. Van Bladel, H. Halen and P. Cloos, *Clay Miner.*, 1993, **28**, 33.
21 S. Miyata, *Clays Clay Miner.*, 1975, **23**, 369.

Paper a906346c